

# A possible formation channel for blue hook stars in globular cluster

Zhenxin Lei<sup>1,2\*</sup>, Xuemei Chen<sup>3</sup>, Fenghui Zhang<sup>2,4</sup> and Zhanwen Han<sup>2,4</sup>

<sup>1</sup>*Department of Science, Shaoyang University, Shaoyang 422000, China*

<sup>2</sup>*Key Laboratory for the Structure and Evolution of Celestial Objects, Chinese Academy of Sciences, Kunming 650011, China*

<sup>3</sup>*Department of Electrical Engineering, Shaoyang University, Shaoyang 422000, China*

<sup>4</sup>*Yunnan Observatory, Chinese Academy of Sciences, Kunming 650011, China*

Accepted ; Received ; in original form

## ABSTRACT

The formation mechanism for blue hook (BHk) stars in globular clusters (GCs) is still unclear. Following one of the possible scenario, named late hot flash scenario, we proposed that tidally enhanced stellar wind in binary evolution may provide the huge mass loss on the red giant branch (RGB) and produce BHk stars. Employing the detailed stellar evolution code, Modules for Experiments in Stellar Astrophysics (MESA), we investigated the contributions of tidally enhanced stellar wind as a possible formation channel for BHk stars in GCs. We evolved the primary stars with different initial orbital periods using the binary module in MESA (version 6208) from zero age main-sequence (ZAMS) to post horizontal branch (HB) stage, and obtained their evolution parameters which are compared with the observation. The results are consistent with observation in the color-magnitude diagram (CMD) and the  $\log g - T_{\text{eff}}$  plane for NGC 2808, which is an example GC hosting BHk stars. However, the helium abundance in the surface for our models is higher than the one obtained in BHk stars. This discrepancy between our models and observation is possibly due to the fact that gravitational settling and radiative levitation which are common processes in hot HB stars are not considered in the models as well as the fact that the flash mixing efficiency may be overestimated in the calculations. Our results suggested that tidally enhanced stellar wind in binary evolution is able to naturally provide the huge mass loss on the RGB needed for late hot flash scenario and it is a possible and reasonable formation channel for BHk stars in GCs.

**Key words:** stars: horizontal branch - binaries: general - globular cluster: individual: NGC 2808

## 1 INTRODUCTION

For a long time, globular clusters (GCs) have been known as the fundamental laboratory for studying stellar structure and evolution, since they are considered to be composed of simple stellar populations (SSP) in which all member stars are formed at the same time with similar chemical abundance. However, this point of view is challenged by recent observations both from photometry and spectroscopy. For example, the splitting of main-sequence (MS) has been found in some massive GCs, such as  $\omega$  Cen (Bedin et al. 2004), NGC 2808 (Piotto et al. 2007) etc. Moreover, star to star variation of light elements (e.g., Na-O, Mg-Al anticorrelation) are found in most of the studied GCs (Carretta et al. 2009; Gratton et al. 2012). Both the splitting of MS and light elements variation in GCs are considered to be possibly related to the self-enrichment scenario with helium enhancement (D’Antona & Caloi 2008; Milone 2015; but also see Jiang et al. 2014 for an alternative solution). In this scenario, the second generation stars are helium enhanced, since they are formed in the material polluted by the ejecta from either massive asymptotic giant branch (AGB) stars (Ventura et al. 2001, 2002) or fast rotating massive stars (Decressin et al. 2007) of the first generation. These second generation stars will occupy a bluer position on MS and horizontal branch (HB) stage than normal stars. In some GCs, the helium abundance for the second generation stars may reach as high as  $Y = 0.4$  (Busso et al. 2007).

Multiple populations in GCs are also found in late stellar evolution stage, such as HB. Recently, Na-O anticorrelation is also discovered in HB stars for many GCs (Gratton et al. 2013, 2014). Marino et al. (2014) analyzed nearly 100 HB stars with different temperatures in NGC

\* E-mail: lzx2008@ynao.ac.cn

2808 and confirmed that some blue HB stars in this GC present higher helium abundance than primordial content by  $\Delta Y = 0.09 \pm 0.01$ . This result provides direct observation constraints on the typical second-parameter problem in GCs which is a long-term puzzle in stellar evolution (see Catelan 2009 for a recent review). In 1960, Sandage & Wallerstein found that the position of HB stars on color-magnitude diagram (CMD), which is defined as HB morphology, is mainly determined by metallicity of GCs. However, other parameters are also needed to explain the diversity of HB morphology in GCs, such as age (Lee et al. 1994; Dotter et al. 2010; Gratton et al. 2010), helium enhancement due to self-enrichment (D’Antona et al. 2002; D’Antona & Caloi 2004; Milone et al. 2014), stellar rotation (Sweigart et al. 1997), binaries (Lei et al. 2013a, 2013b, 2014; Han et al. 2012; Han & Lei 2014), dynamics (Pasquato et al. 2013, 2014), etc.

More complicated situations arise from the discovery for a special population of hot HB stars in some massive GCs, which are called the blue hook (BHK) stars (Whitney et al. 1998; D’Cruz et al. 2000). These stars occupy a very blue position on the HB but with fainter luminosity than the normal extreme horizontal branch (EHB) stars. Due to its high effective temperature (e.g.,  $T_{\text{eff}} \geq 32000$  K; Moni Bidin et al. 2012) and faint luminosity, BHK star can not be explained by canonical stellar evolution theory, and its formation mechanism is still unclear. There are several scenarios having been proposed to explain the formation of BHK stars. Brown et al. (2001) suggested that late hot flash scenario is one of the possible explanations. In this scenario, the helium core flash of low mass stars may take place when the star is descending the white dwarf cooling curve if their progenitors undergo unusually huge mass loss on the red giant branch (RGB) stage. During the helium core flash, hydrogen in the envelope can be mixed into interior and burn into helium at higher temperature. Thus, these stars show helium and carbon enhancement in the surface and occupy a bluer and fainter position than canonical EHB stars in the CMD of GCs. However, the physical mechanism for the huge mass loss on the RGB in late hot flash scenario is still unclear. On the other hand, Lee (2005) suggested that the BHK stars in  $\omega$  Cen and NGC 2808 are likely the progeny of a minority population of bluer and fainter MS stars which could be reproduced by assuming a large variations of primordial helium abundance (e.g.,  $\Delta Y \approx 0.15$ ), while D’Antona et al. (2010) proposed that if the blue MS stars found in  $\omega$  Cen are the progenitors of the BHK stars in this cluster, they need to suffer extra mixing processes on the RGB and increase their surface helium abundance up to  $Y \approx 0.8$ .

In this paper, we followed the late hot flash scenario and suggested that tidally enhanced stellar wind in binary evolution is a possible formation channel for BHK stars in GCs. In binary evolution, the mass loss of a red giant primary star could be largely enhanced by its companion star (Tout & Eggleton 1988), especially when the primary star nearly fills its Roche lobe. In this scenario, the mass loss of the red giant primary star depends on orbital period of the binary system. Some of the primary stars may lost nearly the whole envelope before Roche lobe overflow (RLOF) is taking place due to a relative shorter orbital period. They evolve off the RGB and may experience helium core flash when descending the white dwarf cooling curve (Castellani & Castellani 1993; D’Cruz et al. 1996; Brown et al. 2001, 2010, 2012). After the helium core flash, the star burns helium stably in its core and locates on the BHK regions in CMD of GCs. Employing the detailed stellar evolution code, Modules for Experiments in Stellar Astrophysics (MESA; Paxton et al. 2011, 2013), we investigated the contributions of tidally enhanced stellar wind in binary evolution on the formation of BHK stars in GCs. In Section 2, we introduce the code and models used in this paper. The results and comparison with observations are given in Section 3. Finally, a discussion and conclusion are presented in Section 4 and 5 respectively.

## 2 MODEL CONSTRUCTION

The tidally enhanced stellar wind was firstly suggested by Tout & Eggleton (1988) to explain the mass inversion phenomenon (e.g., more evolved star has a low mass) found in some binaries of RS CVn type (Popper & Ulrich 1977; Popper 1980). They suggested that the secondary star may tidally enhance the stellar wind of the red giant primary star. By considering tidally enhanced stellar wind in binary evolution, they successfully explained the mass of Z Her which is a typical example of system with mass inversion phenomenon. Recently, Lei et al. (2013a, b) also used this kind of wind to explain the HB morphology in GCs, but they did not consider the process of late hot flash and its effects on the formation of BHK stars.

Since the torque due to tidal friction depends on  $(R/R_L)^6$  ( $R$  is the radius of the primary, while  $R_L$  is the Roche lobe radius of the primary. Zahn 1975; Campbell & Papaloizou, 1983), Tout & Eggleton (1988) used the following equation to describe the tidally enhanced stellar wind of the red giant primary:

$$\dot{M} = -\eta 4 \times 10^{-13} (RL/M) \{1 + B_w \times \min[(R/R_L)^6, 1/2^6]\}, \quad (1)$$

where  $\eta$  is the Reimers mass-loss efficiency (Reimers 1975), and  $B_w$  is the efficiency of the tidal enhancement for the stellar wind. Here  $R$ ,  $L$ , and  $M$  are the radius, luminosity and mass of the primary in solar units. Tout & Eggleton introduced a saturation for  $R \geq 1/2 R_L$  in the above expression, because it is expected that the binary system is in complete corotation for  $R/R_L \geq 0.5$ . In this study, we set  $\eta = 0.45$  (Renzini & Fusi Pecci 1988; also see the discussion in Sect 4.2 of Lei et al. 2013b),  $B_w = 10000$  (e.g., a typical value used in Tout & Eggleton 1988).

To study the contribution of tidally enhanced stellar wind on the formation of BHK stars, equation (1) was added into the detailed stellar evolution code, Modules for Experiments in Stellar Astrophysics (MESA; Paxton et al. 2011, 2013). MESA provides a variety of up-to-date physics modules, and it can evolve low mass stars through the helium core flash phase with details. Furthermore, it offers the capacity that users can create zero age main-sequence (ZAMS) and zero age horizontal branch (ZAHB) models with different chemical compositions conveniently. We evolve binary systems using the binary module of MESA, version 6208. In the study, all the default values for input physics in MESA are used except for the opacity tables. OPAL type I opacity tables are the default ones for MESA, but OPAL type II opacity tables

**Table 1.** Main input parameters used in the study.

$M_{\text{ZAMS}}(M_{\odot})$	$Z$	$Y$	$q$	$\eta$	$B_w$
0.83 <sup>a</sup>	0.001	0.24	1.6	0.45	10000

<sup>a</sup> This value of mass corresponds to an age of about 12 Gyr at RGB tip with  $Z = 0.001$  and  $Y = 0.24$ .

allow time dependent variation of C and O abundances independent of initial metal distribution, thus it gives a better approximation of the appropriate opacities during and after helium burning. Therefore, OPAL type II opacity tables are used in this study.

In the calculation, the secondary stars are assumed to be MS stars and the mass ratio of primary to secondary is set to 1.6 (see the discussion in Sect 4 of Lei et al. 2013a for different values of  $q$ ). Since what we concern is the primary star which may become a BHK star after undergoing huge mass loss on the RGB, we do not evolve the secondary star during the binary evolution. In our calculations, a moderate metallicity,  $Z = 0.001$  which is a typical value for GCs in our Galaxy, is adopted, and a primordial helium abundance  $Y = 0.24$  is adopted. In our models, the mass of primary star at ZAMS is  $0.83M_{\odot}$  which corresponds to an age of about 12 Gyr at the RGB tip, and it is consistent with the typical age of GCs. We present in Table 1 the main input parameters described above. From left to right, it gives the mass of primary star at ZAMS, metallicity, helium abundance, mass ratio of primary to secondary, Reimers mass loss efficiency and tidal enhancement efficiency, respectively.

When considering the tidally enhanced stellar wind in binary evolution, the mass loss of the primary star on the RGB depends on the orbital period (Lei et al. 2013a). For a long initial orbital period, the primary may lose little envelope mass due to the weak effects of the secondary and become a normal HB star after helium core flash. On the other hand, for a moderate short period, the primary may lose much or nearly the whole envelope mass and become a canonical EHB or BHK star after helium core flash. However, if the orbital period is short enough, the primary may lose too much envelope mass on the RGB to ignite helium in its core, and it will die as an helium white dwarf. For this reason, four different initial orbital periods are used in our calculation, which are 2200, 2000, 1610 and 1600 in days, respectively. For each period, we evolve the primary star from ZAMS to post HB phase and obtain the evolution parameters of the primary. The results are given in next section.

### 3 RESULTS

In this section, we present the evolution for the primary stars from ZAMS to post HB stage after undergoing huge mass loss on the RGB. To compare our results with the observations in the CMD of GC, the effective temperatures and luminosity of the stars at helium burning stage are transformed into colors and magnitudes using the stellar spectra library compiled by Lejeune et al. (1997, 1998). We also compared our results with the observation in the  $\log g - T_{\text{eff}}$  diagram of NGC 2808.

#### 3.1 Evolution tracks

Fig. 1 gives the evolution tracks of a primary star with an age of about 12 Gyr at RGB tip for different initial orbital periods. The pentacles in this figure denote the position where the primary helium core flash takes place, while the open squares denote the ZAHB positions for each evolution track. In Panel (a), with an initial orbital period of  $P_i = 2200$  d, the primary star undergoes a normal helium core flash at RGB tip, and it becomes a canonical EHB star with  $\log T_{\text{eff}} = 4.33$  and  $\log L/L_{\odot} = 1.24$  at ZAHB after the helium core flash. One can infer simply that if the orbital period is larger than this one, the primary star may lose less envelope mass and locate on redder and more luminous position of HB (see Lei et al. 2013a). For the track with  $P_i = 2000$  d in Panel (b), due to the huge mass loss, the primary star evolves off the RGB tip and undergoes the helium core flash when crossing the H-R diagram. This kind of flash is called the early hot flash (Lanz et al. 2004; Miller Bertolami et al. 2008), in which the flash mixing can not penetrate the envelope and change the surface chemical abundance of the star. After the helium core flash, the primary star for early hot flash locates on a hotter and fainter HB position in H-R diagram with  $\log T_{\text{eff}} = 4.48$  and  $\log L/L_{\odot} = 1.19$ . However, for the track with  $P_i = 1610$  d in Panel (c), helium core flash of the primary star occurs when the star is descending the white dwarf cooling curve, which is called the late hot flash (Lanz et al. 2004; Miller Bertolami et al. 2008). In this case, hydrogen in the envelope can be mixed into helium burning interior by the flash triggered mixing. Therefore, the surface of this kind of star is helium and carbon enhanced (Cassisi et al. 2003), and the star locates on the BHK position with highest temperature and faintest luminosity in H-R diagram (e.g.,  $\log T_{\text{eff}} = 4.55$  and  $\log L/L_{\odot} = 1.16$ ). In panel (d), with an initial orbital period of  $P_i = 1600$  d, the primary star fails to ignite helium in the core due to too much mass loss on the RGB, and it dies as an helium white dwarf. Obviously, any periods shorter than this one would produce helium white dwarfs rather than HB stars due to the too much mass loss on the RGB.<sup>1</sup>

We also give in Table 2 the evolution parameters at ZAHB for the tracks shown in Fig. 1. From left to right of Table 2, it presents

<sup>1</sup> In our models, we do not consider close binaries in which the primary may fill its Roche lobe on the RGB and transfer envelope to the secondary rapidly and form EHB stars (see Han et al. 2002, 2003).

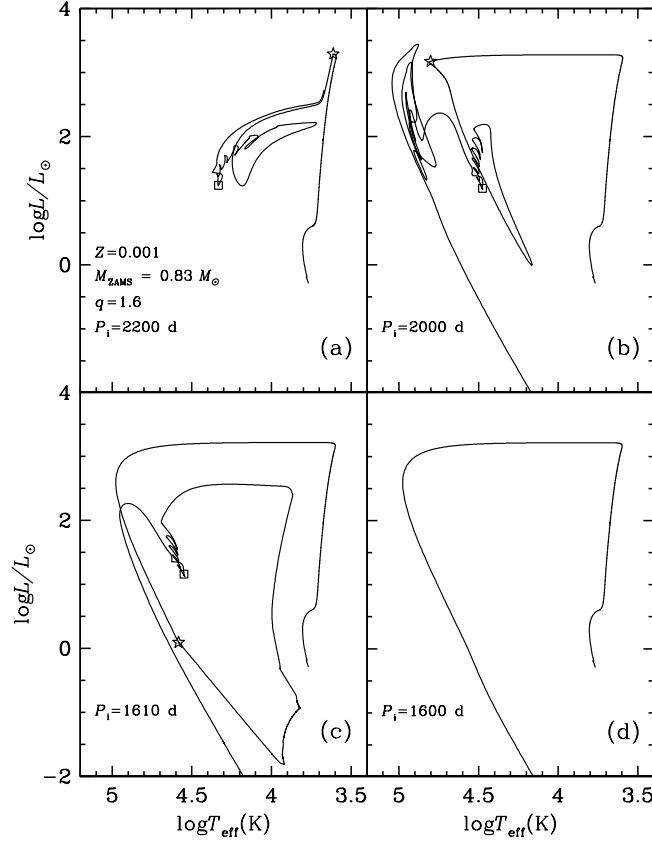


**Figure 1.** The evolution tracks for the primary star undergoing tidally enhanced stellar wind. The pentacles in each panel represent the position where the primary helium core flash takes place, while the open squares denote ZAHB position. The initial orbital periods are labeled in each panel.

**Table 2.** Evolution parameters at ZAHB for the tracks shown in Fig.1

$P_i$ (days)	$M_{\text{ZAHB}}(M_{\odot})$	$M_{\text{core}}(M_{\odot})^a$	$\log T_{\text{eff}}$	$\log L/L_{\odot}$	$\log g$	$X_{\text{surf}}$	$Y_{\text{surf}}$	$C_{\text{surf}}$	Flash status
2200 <sup>b</sup>	0.5036	0.4817	4.3323	1.2393	5.1833	0.7443	0.2531	$1.6144 \times 10^{-4}$	normal
2000 <sup>c</sup>	0.4829	0.4814	4.4756	1.1941	5.7837	0.7443	0.2531	$1.6161 \times 10^{-4}$	early
1610	0.4702	0.4702	4.5498	1.1593	6.1035	0.0014	0.9701	$1.0676 \times 10^{-2}$	late
1600 <sup>d</sup>	—	—	—	—	—	—	—	—	WD

<sup>a</sup> The helium core mass is defined by the region in which the hydrogen mass fraction is lower than 0.01.

<sup>b</sup> The minimum initial orbital period for the normal helium core flash at the RGB tip (see text for detail).

<sup>c</sup> The minimum initial orbital period for early hot flash (see text for detail).

<sup>d</sup> Any initial periods shorter than this one would produce helium white dwarfs due to too much mass loss on the RGB.

the initial orbital period, stellar mass, helium core mass, effective temperature, luminosity, gravity, surface hydrogen mass fraction, surface helium mass fraction, surface carbon mass fraction and the flash status (e.g., what kind of flash does the primary star experience, 'normal' means the star experiences a normal helium core flash at the RGB tip, 'early' means it experiences an early hot flash when crossing the H-R diagram, 'late' means it experiences a late hot flash when descending the white dwarf cooling curve, while 'WD' means the primary star fails to ignite helium and dies as an helium white dwarf). One can see from Table 2 that with the decreasing of initial orbital periods for the binaries, more envelope mass of the primary star is lost due to tidally enhanced stellar wind. Though the early hot flasher (e.g.,  $P_i = 2000$  d) shows a little smaller helium core mass than the normal flasher (e.g.,  $0.4814 M_{\odot}$  vs  $0.4817 M_{\odot}$ ), its envelope mass is much less than the normal one (e.g.,  $0.0015 M_{\odot}$  vs  $0.0219 M_{\odot}$ ). Thus, it results in a difference of about 8400 K for the ZAHB temperature between early hot flasher and normal flasher. However, the mass fractions of hydrogen, helium and carbon in the surface both for the early hot flasher and the normal one are nearly the same, which means that the chemical compositions in the surface of the two models are not changed by the helium core flash process. On the other hand, due to loss of nearly the whole envelope mass on the RGB, the late hot flasher (i.e.,  $P_i = 1610$  d) presents the smallest helium core mass and the thinnest envelope mass at ZAHB when comparing with the early hot flasher and

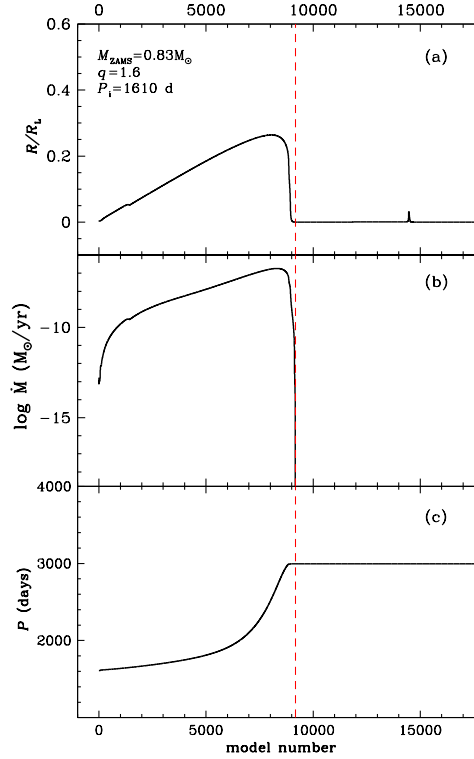


**Figure 2.** Binary evolution parameters vs model number. Model number is the time step calculated in MESA. The red-dashed line denotes the time when the primary helium core flash is taking place. Panel (a), (b) and (c) gives the evolution of the ratio between radius and Roche lobe radius, mass loss rate in stellar wind and orbital period, respectively.

the normal flasher. As predicted by Brown et al. (2001), the late hot flasher in Table 2 shows hydrogen deficiency but helium and carbon enhancement in the surface. Due to the highest helium abundance in the surface (e.g., 0.97 by mass) and thinnest envelope mass, the late hot flasher presents highest effective temperature at ZAHB which is higher than early hot flasher about 5500 K and is higher than normal flasher for about 14000K. Since the primary for  $P_i = 1600$  d becomes an helium white dwarf, we do not give the parameters for this model in Table 2.

According to our calculations,  $P_i = 2200$  d is the minimum initial orbital period for which the primary stars would experience normal helium core flash at the RGB tip, while  $P_i = 2000$  d is the minimum initial orbital period for which the primary stars would experience early hot flash. That is to say, if the initial orbital periods are longer than  $P_i = 2200$  d, the primary stars would experience normal helium core flash at the RGB tip and become canonical HB stars (e.g., EHB, blue HB or red HB stars, see Lei et al. 2013a), while if the initial orbital periods are shorter than  $P_i = 2200$  d but longer than  $P_i = 2000$  d, the primary stars would experience early hot flash and become normal EHB stars. For  $1600 \text{ d} < P_i < 2000 \text{ d}$ , the primary stars would undergo late hot flash when descending the white dwarf cooling curve and become BHK stars. However, if the initial orbital periods are shorter than  $P_i = 1600$  d, the primary stars would fail to ignite helium in the core due to too much mass loss on the RGB and become helium white dwarfs.

Cassisi et al. (2003) firstly presented the evolution of a metal-poor low mass star from ZAMS to post HB phase through a delayed helium core flash when the star is descending the white dwarf cooling curve. In their models, stars lose envelope mass on the RGB through Reimers mass-loss law (Reimers 1975). For the model undergoing late hot flash (e.g.,  $\eta = 0.60$  in Cassisi et al. 2003), the mass fraction of hydrogen, helium and carbon in the surface is  $4 \times 10^{-4}$ , 0.96 and 0.029 respectively. For our model in Table 2 with an initial orbital period of  $P_i = 1610$  d, which also experienced a late hot flash, the surface hydrogen, helium and carbon mass fraction are  $1.4 \times 10^{-3}$ , 0.97 and 0.011 respectively. The slight difference for chemical abundance in surface between the model in Cassisi et al. (2003) and ours may be due to the different mixing efficiency of the convective region used in the two model calculations (also see the comparison in Table 4 of Miller Bertolami et al. 2008 between their results and the ones in Cassisi et al. 2003).

In figure 2, we give the evolution parameters for one of our binary systems from ZAMS to post HB, in which initial orbital period  $P_i = 1610$  d. The red-dashed line in Fig. 2 denotes the time when the primary helium core flash is taking place. Panel (a) shows the ratio of stellar

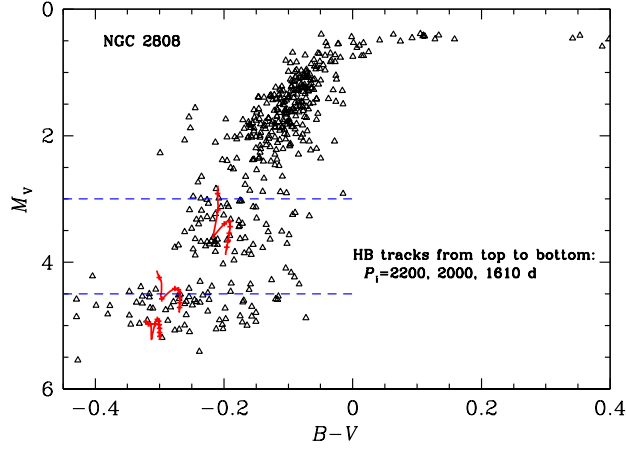


**Figure 3.** Comparing the evolution tracks at helium burning stage shown in Fig. 1 with observation in the CMD of NGC 2808. The mass of the primary at ZAMS is  $0.83M_{\odot}$ , the mass ratio of primary to secondary is 1.6,  $Z = 0.001$ . From top to bottom, the initial orbital periods for the evolution tracks are  $P_i = 2200, 2000$  and  $1610$  days. The time interval between two adjacent + symbols in each track is  $10^7$  yr. The top blue-dashed line at  $M_V = 3^m$  roughly distinguishes canonical EHB stars from classical blue HB stars, while the bottom blue-dashed line at  $M_V = 4^m.5$  roughly distinguishes BHk stars from canonical EHB stars (see the text for details). The photometric data for NGC 2808 is from Piotto et al. (2002).

radius to Roche lobe radius for the primary star vs model number<sup>2</sup>. One can see from Panel (a) that the envelope of the primary star expands from ZAMS and gradually closes to the Roche lobe radius until it reaches the RGB tip. According to equation (1), mass loss from tidally enhanced stellar wind become more and more stronger when the radius of the primary star is being closer to its Roche lobe radius. This process is apparently shown in Panel (b), which gives the evolution of mass loss rate in logarithms (i.e.,  $\log \dot{M} M_{\odot}/\text{yr}$ ) for the primary star. Due to the huge mass loss on the RGB, the star contracts and evolves off the RGB tip. At the same time, the mass loss of the star decreases accordingly. When the primary helium core flash takes place on the white dwarf cooling curve, we shut down the stellar wind of the star. One can see from Panel (a), there is a small second expansion for the radius of the star beyond the RGB tip. This is due to the fact that the hydrogen in the envelope was mixed into the inner region during the helium core flash and burned into helium at high temperature, which released large quantities of energy and push the envelope towards lower temperatures. Panel (c) in Fig. 2 shows the period evolution of the binary vs model number. The orbital period of the binary becomes more and more longer until the star reaches the RGB tip (e.g., from 1610 d at ZAMS to about 3000 d at the RGB tip) due to the mass loss and angular momentum loss from the primary star. After the star evolving off the RGB tip, mass loss and angular momentum loss decrease largely, thus it changes the orbital period a little.

### 3.2 Comparison with observation for NGC 2808

Brown et al. (2001) discovered the BHk populations in the ultraviolet CMD of NGC 2808. This cluster is one of the most massive globular clusters in our Galaxy with an intermediate metallicity of  $Z = 0.0014$  (i.e.,  $[\text{Fe}/\text{H}] = -1.15$ , Harris 1996, version 2003) and an age of  $11 \pm 0.38$  Gyr (VandenBerg et al. 2013). Since the parameters of GC NGC 2808 are similar with the ones used in our model calculations, we compare our results with this cluster in the CMD and  $\log g - T_{\text{eff}}$  plane. To compare our results with the observation in CMD, the effective temperatures and luminosity of each evolution track shown in Fig. 1 are transformed into colors and absolute magnitudes using the stellar spectra library compiled by Lejeune et al. (1997, 1998).

Fig. 3 shows the comparison of our evolution tracks with the observation in the CMD of NGC 2808. The photometric data for this cluster is obtained by Piotto et al. (2002) with the HST/WFPC2 camera in the F439W and F555W bands. The magnitudes in F439W and F555W bands are transformed into standard Johnson  $B$  and  $V$  magnitudes by Piotto et al. (2002) using an iterative procedure (see Sect 2.4 in their study). The distance module for the cluster is set to 15.25 and the reddening correction  $E(B - V)$  is set to 0.18 in Fig. 3 (Bedin et al. 2000; D’Antona & Caloi 2004). According to previous study for this cluster, there are two apparent gaps on the blue tail of NGC 2808 at  $M_V \approx 3^m$  and  $4^m.5$  (Bedin et al. 2000; Moehler et al. 2004). The brighter gap distinguishes canonical EHB stars from classical blue HB stars (e.g., denoted by the top blue-dashed line in Fig. 3; Moehler et al. 1997, 2000; Momany et al. 2002), while the fainter gap separates BHk stars from canonical EHB stars (e.g., denoted by the bottom blue-dashed line in Fig. 3; Brown et al. 2001; Moehler et al. 2004).

<sup>2</sup> Model number is the time step calculated in MESA and therefore not proportional to time.

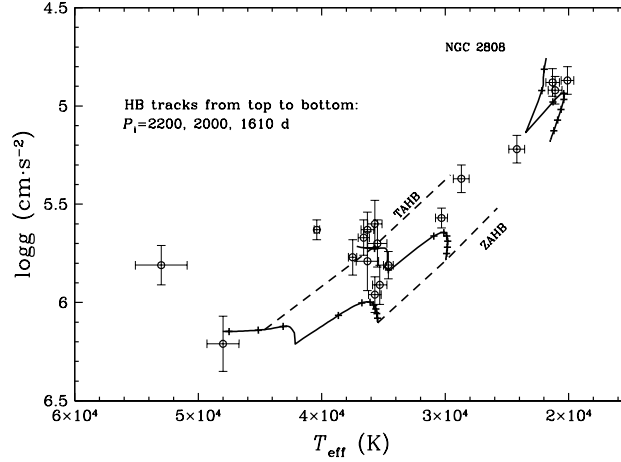


**Figure 4.** Comparing the HB evolution tracks shown in Fig. 3 with observation in the  $\log g - T_{\text{eff}}$  plane for NGC 2808. The atmospheric parameters for BHk stars in NGC 2808 are from Moehler et al. (2004). The time interval between two adjacent + symbols in each track is  $10^7$  yr. The two dashed lines at bottom and top denote the ZAHB and TAHB positions (see the text for details).

In Fig. 3, open triangles represent the observational HB stars in NGC 2808<sup>3</sup>, while the three red-solid curves are the evolution tracks at helium burning stage shown in Fig. 1. From top to bottom, the initial orbital periods for the evolution tracks are  $P_i = 2200, 2000, 1610$  d respectively. The time interval between two adjacent + symbols in each track is  $10^7$  yr. For the top evolution track with  $P_i = 2200$  d, the primary star undergoes a normal helium core flash at the RGB tip and locates on the canonical EHB regions in the CMD (e.g., brighter than  $M_V \approx 4^m$  but fainter than  $M_V \approx 3^m$ ). The middle evolution track with  $P_i = 2000$  d undergoes an early hot flash and presents a little bit smaller helium core mass but much thinner envelope mass than the top one (e.g.,  $P_i = 2200$  d, see Table 2). Therefore, it occupies a bluer and fainter region than the top evolution track in the CMD (e.g., nearby the region for  $M_V \approx 4^m.5$ ). Obviously, both the normal and the early hot flash track cannot reach the faintest region in the CMD which is occupied by BHk stars. On the other hand, for the evolution track with  $P_i = 1610$  d, it experiences a late hot flash and show the smallest helium core mass as well as highest helium abundance in the surface and locates well on the BHk regions in the CMD.

### 3.3 $\log g - T_{\text{eff}}$ plane

Fig. 4 shows the comparison between our evolution tracks and the observation in  $\log g - T_{\text{eff}}$  plane for NGC 2808. In this figure, the open circles denote the BHk and canonical EHB stars in NGC 2808 analyzed by Moehler et al. (2004). As the same with Fig. 3, the three solid curves in this figure are the evolution tracks with initial orbital periods of  $P_i = 2200, 2000, 1610$  d from top to bottom, which correspond to normal flasher, early hot flasher and late hot flasher respectively. The dashed line at the bottom denotes the ZAHB positions, while the dashed line at the top denotes the terminal age HB (TAHB) positions (TAHB is defined by the stage when central helium abundance has dropped below 0.0001 in mass fraction).

Comparing with the evolution tracks, one can see in Fig. 4 that the stars with  $T_{\text{eff}} \lesssim 32000$  K are canonical EHB stars which are most likely formed through normal or early hot helium flash. On the other hand, most of the BHk stars with  $T_{\text{eff}} > 32000$  K (Moehler et al. 2004; Moni bidin et al. 2012) are well predicted by the late hot flash track for  $P_i = 1610$  d. As discussed in Moehler et al. (2004), the two hottest stars with  $T_{\text{eff}} > 45000$  K may be post HB stars which have exhausted helium in the cores and evolve towards the white dwarf cooling curve. One would be aware of that the gravities for BHk stars obtained by Moehler et al. (2004) seems to be generally lower than the ones predicted by our late hot flash track. This discrepancy between observation and model calculation also seems appear in Fig. 5 of Moehler et al. (2004). A possible explanation for this discrepancy is that the late hot flash scenario predicts enrichment in carbon and nitrogen (Lanz et al. 2004), while this enrichment is not considered in the model atmospheres when obtaining the atmospheric parameters for BHk stars in NGC 2808. However, Moehler et al. (2011) obtained two sets of atmospheric parameters for the He-rich hot HB stars in  $\omega$  Cen with and without considering carbon and nitrogen enrichment in the model atmospheres. By comparing the two sets of gravities list in Table 4 of Moehler et al. (2011), one can infer that the gravities obtained with C/N enhanced model atmospheres are generally larger than the ones obtained without C/N enhanced model atmospheres by a mean value of about 0.13 dex. Therefore, a better match between the observation and model calculation would be expected if the enrichment of carbon and nitrogen is considered in the model atmospheres to obtain the atmospheric parameters for BHk stars in NGC 2808 (also see the discussion in Sect 4.4 of Moni Bidin et al. 2012).

<sup>3</sup> The red HB stars in this GC are not shown for clarity.

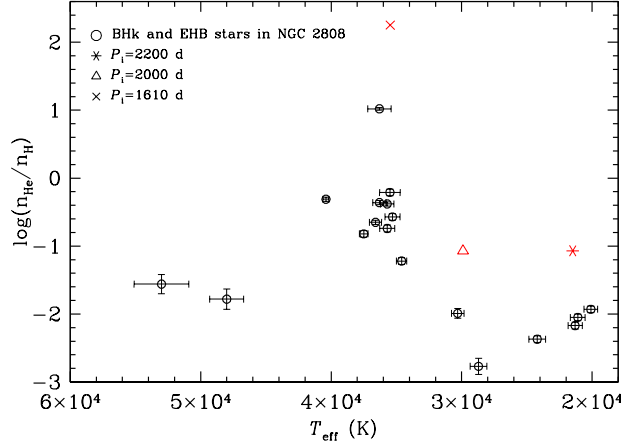


**Figure 5.** Comparing helium abundance between our models at ZAHB and the BHk stars of NGC 2808 in  $\log(n_{\text{He}}/n_{\text{H}}) - T_{\text{eff}}$  plane. The observation data is from Moehler et al. (2004).

#### 4 DISCUSSION

Moehler et al. (2004) analyzed medium resolution spectra for some BHk stars in NGC 2808 and obtained their atmospheric parameters, including the surface helium abundance. Therefore, we compare our results with the observation in the  $\log(n_{\text{He}}/n_{\text{H}}) - T_{\text{eff}}$  plane of NGC 2808 in Fig. 5. In this figure, open circles are BHk stars or canonical EHB stars in NGC 2808 analyzed by Moehler et al. (2004), while asterisk, open triangle and cross denote our ZAHB models for normal flasher, early hot flasher and late hot flasher respectively. As seen in Fig. 5, our ZAHB models which undergo normal flash and early hot flash (e.g., asterisk and open triangle) show higher helium abundance than the stars in NGC 2808 with similar effective temperatures (e.g., in the range of 20000 K  $\sim$  32000 K). As discussed in Sect 3, these stars are most likely the canonical EHB stars and may have normal chemical composition in the surface but undergo gravitational settling and radiative levitation (Grundahl et al. 1999; Moehler et al. 2004; Miller Bertolami et al. 2008) which may lead to a helium poor and hydrogen rich surface. However, these processes are not considered in our models, and it may causes the discrepancy in helium abundance between our models and the observation shown in Fig. 5. Except for the two hottest stars in Fig. 5 (e.g.,  $T_{\text{eff}} > 45000$  K), all the BHk stars in NGC 2808 with  $T_{\text{eff}} > 32000$  K show solar or super solar helium abundance<sup>4</sup>. This result is consistent with the late hot flash scenario which predicts a helium enhancement in the surface. However, our ZAHB model for late hot flash shows a value of  $\log(n_{\text{He}}/n_{\text{H}}) \approx 2.23$  (e.g., the cross in Fig. 5), which is higher than the most He-rich BHk star in NGC 2808 (e.g.,  $\log(n_{\text{He}}/n_{\text{H}}) \approx 1$ ) by about 1.2 dex. A similar discrepancy also appeared in Cassisi et al. (2003) when they compared their results with the BHk stars observed in  $\omega$  Cen. A value of  $\log(n_{\text{He}}/n_{\text{H}}) \approx 2.8$  is obtained for the late hot flash model in Cassisi et al. (2003), while the highest helium abundance for BHk stars in  $\omega$  Cen obtained by Moehler et al. (2002) is  $\log(n_{\text{He}}/n_{\text{H}}) \approx 0.94$ . Cassisi et al. (2003) suggested that a reduction by a factor of  $2 \times 10^4$  for mixing efficiency would increase the residual of hydrogen by an order of magnitude. Similarly, this explanation is a possible solution for the discrepancy presented here, which means that the flash mixing efficiency may be overestimated in our model calculation. On the other hand, Moehler et al. (2004) proposed another possible solution that this discrepancy could be explained if some hydrogen survived the flash mixing and late diffused outward into the surface. Miller Bertolami et al. (2008) estimated that the time scale of such a diffusive processes is about  $10^6$  yr, which is much shorter than the HB life time of about  $10^8$  yr.

The late hot flash scenario also predicts a carbon enhancement in the surface of BHk stars (Brown et al. 2001). In the study of Moehler et al. (2007), the surface abundance for helium, carbon and nitrogen were obtained for BHk stars and canonical EHB stars in  $\omega$  Cen. They found that carbon enrichment strongly correlated with helium enrichment, e.g., with carbon enhancement of at least 1% up to 3% by mass for the He-rich stars (see Fig. 3 in Moehler et al. 2007). Moreover, Latour et al. (2014) obtained the spectra of 38 hot EHB stars ( $T_{\text{eff}} > 30000$  K) in  $\omega$  Cen using the MXU mode of FORS2/VLT and determined their fundamental parameters (e.g., effective temperature, gravity, surface abundance for hydrogen, helium and carbon). They clearly found that there is a positive correlation between carbon and helium enrichment for their He-rich EHB stars (see Fig. 7 in Latour et al. 2014), and the surface carbon mass fraction is up to about 1.5% for the most He-rich EHB stars. These observations are consistent with the results predicted by our late hot flash model in this study (e.g., in Table 2, the surface carbon for the late hot flash model is about 1.1% by mass, which is nearly two orders of magnitude higher than the value for normal flash and early hot flash model), and it seems to favor the late hot flash scenario for the formation of He-rich EHB stars in  $\omega$  Cen (but also see the discussion in Sect 4.2 of Latour et al. 2014).

BHk stars have been so far found in a few most massive GCs. Dieball et al. (2009) investigated the relationship between the physical or structural parameters of GCs and the presence of BHk stars. They found that the mass of GCs is the most important fact linked to the

<sup>4</sup> In Fig.5,  $\log(n_{\text{He}}/n_{\text{H}}) = -1$  denotes the solar helium abundance.



formation of BHk stars when comparing the GCs with and without BHk stars. A possible solution for this result is that more massive GCs host more binaries, and the binary interaction (e.g., tidally enhanced stellar wind) may provide the huge mass loss on the RGB which is needed for the late hot flash scenario to form BHk stars. From Table 1 of Dieball et al. (2009), the GCs hosting BHk stars also show long relaxation times, large core radii, small concentration and large escape velocities, which means these GCs are not core-collapsed. The most likely explanation is that a significant fraction of binaries exist in these GCs and decelerate or prevent the core collapse process.

Recently, low close binary fraction was found for EHB stars in GCs (Moni Bidin et al. 2008, 2011), which demonstrated a different formation channel between EHB stars and their counterparts in the field, subdwarf B (sdB) stars (Han et al. 2002, 2003). This result does not contradict with ours. One can see from Table 2 in this study, the initial orbital periods of the binaries which can produce BHk stars or canonical EHB stars by tidally enhanced stellar wind are longer than 1000 d. Moreover, the orbital periods of the binary become even longer during the binary evolution (see Panel (c) in Fig. 2). Thus, it is difficult for these systems to be identified as binaries from observation. Radial velocity (RV) survey is likely unable to find these binaries as well due to their long orbital periods, since the RV variations for these systems would be too small. However, some of these binaries may be detected by eclipses, though long campaigns would be required. In our models, the secondary is a MS star which is not too faint (e.g.,  $0.52M_{\odot}$  for  $q = 1.6$ ). If this is the case, the BHk primary star could be redder and more luminous than as a single hot HB star in the optical CMD of GCs. In fact, Castellani et al. (2006) found some peculiar HB stars (named HBp stars in their study) which are cooler or redder than the typical hot HB stars in the optical CMD of NGC 2808 (see Fig. 2 in Castellani et al. 2006), and they suggested that at least a fraction of these stars are a binary nature with the faint companions having not been detected. On the other hand, Bedin et al. (2000) and Iannicola et al. (2009) found no distinct radial distribution differences for HB stars (including EHB stars) in NGC 2808, which argues against the binary nature for these stars. Since binary systems would be segregated into the core of the GC due to their massive masses, the BHk stars would be more central concentrated if they are formed through binaries. One roughly possible explanation for this contradiction is that the BHk primary stars may be diffused out the GC's core by exchange interactions during the evolution of the cluster. Due to the high density in the core of GCs, there are short-lived three and four-body gravitational encounters where a star may be exchanged into an existing binary and displaces one of the components of that binary (Heggie 1975). By doing N-body simulations for 100,000 stars in cluster, Hurley et al. (2007) found that the primordial binaries can be replaced by new dynamical or exchange binaries through exchange interaction, and these exchange binaries even become a dominate population in the core of GC at the core-collapse phase (see Fig. 7 in their study).

The tidal enhancement efficiency,  $B_w$ , in this study is set to 10000 which is a typical value used by Tout & Eggleton (1988), but a different value of  $B_w$  will not influence much on the main results obtained in this study (see the discussion in Lei et al. 2013a). Since a smaller  $B_w$  would cause enough mass loss on the RGB and produce BHk stars for a relative shorter period, while a bigger one also would produce BHk stars with a relative longer period. Though a fixed value for the mass ratio of primary to secondary is used in this study (e.g.,  $q = 1.6$ ), as discussed in Lei et al. (2013a), we found limited effects for different values of  $q$  on the mass loss of the primary star, and it just alters a little bit of the initial binary period which is needed to produce BHk stars. Finally, it is worth mentioning that, though the parameters used in this study are suitable for GCs (e.g., age, metallicity), the scenario proposed here (i.e., the tidally enhanced stellar wind) is also a possible explanation for the formation of hot subdwarf stars in the field, which has been previously suggested by Han et al. (2010), but the detailed investigation for this field is out the scope of current study.

## 5 CONCLUSIONS

In this paper, we suggested that tidally enhanced stellar wind in binary evolution may provide the huge mass loss on the RGB which is needed for the late hot flash scenario to explain the formation of BHk stars. The tidally enhanced stellar wind was added into detailed stellar evolution code, MESA, to investigate its contributions on the formation of BHk stars. Four different initial orbital periods for binaries are adopted in the calculations, e.g.,  $P_1 = 2200, 2000, 1610$  and  $1600$  days. We found that, if the initial orbital period are longer than  $P_1 = 2200$  d, the primary stars would experience normal helium flash at the RGB tip and become canonical HB stars, e.g., EHB, blue HB or red HB stars, while if the initial periods are shorter than  $P_1 = 2200$  d but longer than  $P_1 = 2000$  d, the primary stars would experience early hot flash and become canonical EHB stars. For  $1600 \text{ d} < P_1 < 2000 \text{ d}$ , the primary stars undergo late hot flash when descending the white dwarf cooling curve and become BHk stars after helium core flash. However, if the initial orbital periods are shorter than  $P_1 = 1600$  d, the primary stars would become helium white dwarfs due to too much mass loss on the RGB. Our results are consistent with the observation in the CMD and the  $\log g - T_{\text{eff}}$  plane for NGC 2808. However, the helium abundance of our models seems to be higher than the ones observed in BHk stars. It may be due to the fact that gravitational settling and radiative levitation are not considered in our models as well as the fact that flash mixing efficiency is overestimated in the calculation. The orbital periods for the binary systems that can produce BHk stars or canonical EHB stars by tidally enhanced stellar wind may be too long to make these systems identified as binaries in observation. Our results suggested that tidally enhanced stellar wind in binary evolution is a possible and reasonable formation channel for BHk stars in GCs.

## ACKNOWLEDGMENTS

It is a pleasure to thank the referee, Christian Moni Bidin, for his valuable suggestions and comments, which improved the manuscript greatly. This work is supported by the Key Laboratory for the Structure and Evolution of Celestial Objects, Chinese Academy of Science (OP201302).

Z. H. is partly supported by the Natural Science Foundation of China (Grant No. 11390374), the Science and Technology Innovation Talent Programme of the Yunnan Province (Grant No. 2013HA005) and the Chinese Academy of Sciences (Grant No. XDB09010202).

## REFERENCES

- Bedin, Luigi R., Piotto, Giampaolo., Anderson, Jay. et al., 2004, *ApJ*, 605, L125
- Bedin, L. R., Piotto, G., Zoccali, M. et al., 2000, *A&A*, 363, 159
- Brown, T. M., Lanz, T., Sweigart, A. V. et al., 2012, *ApJ*, 748, 85
- Brown, T. M., Sweigart, A. V., Lanz, T. et al., 2001, *ApJ*, 562, 368
- Brown, T. M., Sweigart, A. V., Lanz, T. et al., 2010, *ApJ*, 718, 1332
- Busso, G., Cassisi, S., Piotto, G. et al., 2007, *A&A*, 474, 105
- Campbell, C. G., & Papaloizou, J., 1993, *MNRAS*, 204, 433
- Carretta, E., Bragaglia, A., Gratton, R., Lucatello, S., 2009, *A&A*, 505, 139
- Cassisi, S., Schlattl, H., Salaris, M., & Weiss, A., 2003, *ApJ*, 582, L43
- Castellani, M., & Castellani, V., 1993, *ApJ*, 407, 649
- Castellani, V., Iannicola, G., Bono, G. et al., 2006, *A&A*, 446, 569
- Catelan, M., 2009, *ApSS*, 320, 261
- D'Antona, F., & Caloi, V., 2008, *MNRAS*, 390, 693
- D'Antona, F., & Caloi, V., 2004, *ApJ*, 611, 871
- D'Antona, F., Caloi, V., & Ventura, P., 2010, *MNRAS*, 405, 2295
- D'Antona, F., Caloi, V., Montalbán, J., Ventura, P., & Gratton, R., 2002, *A&A*, 395, 69
- D'Cruz, N. L., Dorman, B., Rood, R. T. et al., 2000, *ApJ*, 530, 352
- D'Cruz, N. L., Dorman, B., Rood, R. T., & O'Connell, R. W., 1996, *ApJ*, 466, 359
- Decressin, T., Meynet, G., Charbonnel, C. et al., 2007, *A&A*, 464, 1029
- Dieball, A., Knigge, C., Maccarone, T. J. et al., 2009, *MNRAS*, 394, L56
- Dotter, A., Sarajedini, A., Anderson, J. et al., 2010, *ApJ*, 708, 698
- Gratton, R. G., Carretta, E., Bragaglia, A. et al., 2010, *A&A*, 517, A81
- Gratton, R. G., Carretta, E., & Bragaglia, A., 2012, *A&ARv*, 20, 50
- Gratton, R. G., Lucatello, S., Sollima, A. et al., 2013 *A&A*, 549, A41
- Gratton, R. G., Lucatello, S., Sollima, A. et al., 2014 *A&A*, 563, A13
- Han, Z., Chen, X., & Lei, Z. 2010, *AIPC*, 1314, 85
- Han, Z., Chen, X., Lei, Z., & Podsiadlowski, P., 2012, *ASPC*, 452, 3
- Han, Z. W., & Lei, Z. X., 2014, *ASPC*, 481, 213
- Han, Z., Podsiadlowski, Ph., Maxted, P. F. L., & Marsh, T. R., 2003, *MNRAS*, 341, 669
- Han, Z., Podsiadlowski, Ph., Maxted, P. F. L., Marsh, T. R., & Ivanova, N., 2002, *MNRAS*, 336, 449
- Harris, W. E., 1996, *AJ*, 112, 1487
- Heggie, D. C. 1975, *MNRAS*, 173, 729
- Hurley, J. R., Aarseth, S. J., & Shara, M. M. 2007, *ApJ*, 665, 707
- Iannicola, G., Monelli, M., Bono, G. et al., 2009, *ApJL*, 696, L120
- Jiang, D. K., Han, Z. W., & Li, L. F., *ApJ*, 2014, 789, 88
- Lanz, T., Brown, T., Sweigart, A., Hubeny, I., & Landsman, W., 2004, *ApJ*, 602, 342
- Latour, M., Randall, S. K., Fontaine, G., Bono, G., Calamida, A., & Brassard, P., 2014, *ApJ*, 795, 106
- Lee, Y.-W., 2005, *ApJ*, 621, L60
- Lee, Y. W., Demarque, P., & Zinn, R., 1994, *ApJ*, 423, 248
- Lei, Z. X., Chen, X. F., Zhang, F. H., & Han, Z. W., 2013a, *A&A*, 549, A145
- Lei, Z. X., Chen, X. M., Zhang, F. H., & Han, Z. W., 2014, *PASJ*, 66, 82
- Lei, Z. X., Zhang, F. H., Ge, H. W., & Han, Z. W., 2013b, *A&A*, 554, A130
- Lejeune, T., Cuisinier, F., & Buser R., 1997, *A&AS*, 125, 229
- Lejeune, T., Cuisinier, F., & Buser R. 1998, *A&AS*, 130, 65
- Marino, A. F., Milone, A. P., Przybilla, N. et al., 2014, *MNRAS*, 437, 1609
- Miller Bertolami, M. M., Althaus L. G., Unglaub, K., & Weiss, A., 2008, *A&A*, 253, 265
- Milone, A. P., 2015, *MNRAS*, 446, 1672
- Milone, A. P., Marino, A. F., Dotter, A. et al., 2014, *ApJ*, 785, 21
- Moehler, S., Dreizler, S., Lanz, T. et al., 2007, *A&A*, 575, L5
- Moehler, S., Dreizler, S., Lanz, T. et al., 2011, *A&A*, 526, A136
- Moehler, S., Heber, U., & Rupprecht, G., 1997, *A&A*, 319, 109

- Moehler, S., Sweigart, A. V., Landsman, W. B., & Heber, U., 2000, A&A, 360, 120
- Moehler, S., Sweigart, A. V., Landsman, W. B. et al., 2004, A&A, 415, 313
- Momany, Y., Piotto, G., Recio-Blanco, A. et al., 2002, ApJ, 576, L65
- Moni Bidin, C., Catelan, M., & Altmann, M. 2008, A&A, 480, L1
- Moni Bidin, C., Villanova, S., Piotto, G., & Momany, Y., 2011, A&A, 528, A127
- Moni Bidin, C., Villanova, S., Piotto, G. et al., 2012, A&A, 547, A109
- Pasquato, M., Raimondo, G., Brocato, E. et al., 2013, A&A, 554, A129
- Pasquato, M. et al., 2014, ApJ, 789, 28
- Paxton, B., Bildsten, L., Dotter, A. et al., 2011, ApJS, 192, 3
- Paxton, B., Cantiello, M., Arras, P. et al., 2013, ApJS, 208, 4
- Piotto, G., Bedin, L. R., Anderson, J. et al., 2007, ApJ, 661, L53
- Piotto, G., King, I. R., Djorgovski, s. G. et al., 2002, A&A, 391, 945
- Popper, D. M., 1980, ARA&A, 18, 115
- Popper, D. M., & Ulrich, R. K., 1977, ApJ, 212, L131
- Reimers, D., 1975, MSRSL, 8, 369
- Sandage, A., & Wallerstein, G., 1960, ApJ, 131, 598
- Sweigart, A. V., 1997, ApJ, 474, L23
- Tout, C. A., & Eggleton, P. P., 1988, MNRAS, 231, 823
- VandenBerg, Don A., Brogaard, K., Leaman, R., Casagrande, L., 2013, ApJ, 775, 134
- Ventura, P., D'Antona, F., Mazzitelli, I., & Gratton, R., 2001, ApJ, 550, L65
- Ventura, P. et al., 2002, A&A, 393, 215
- Whitney, J. H., Rood, R. T., O'Connell, R. W. et al., 1998, ApJ, 495, 284
- Zahn, J. -P., 1975, A&A, 57, 383